Identification of the β^+ Isovector Spin Monopole Resonance via the ^{208}Pb and ^{90}Zr($t, ^3$He) Reactions at 300 MeV/u

K. Miki,[1,2,*,†] H. Sakai,[1,2] T. Uesaka,[3] H. Baba,[2] C. L. Bai,[4] G. P. A. Berg,[5] N. Fukuda,[2] D. Kameda,[2] T. Kawabata,[6]
S. Kawase,[3] T. Kubo,[2] S. Michimasa,[3] H. Miya,[3] S. Noji,[1] T. Ohnishi,[2] S. Ota,[3] A. Saito,[3] Y. Sasamoto,[3] H. Sagawa,[7]
M. Sasano,[2] S. Shimoura,[3] H. Takeda,[2] H. Tokieda,[3] K. Yako,[1] Y. Yanagisawa,[2] and R. G. T. Zegers[8]

[1]*Department of Physics, University of Tokyo, 7-3-1 Hongo, Bunkyo, Tokyo 113-0033, Japan*
[2]*RIKEN Nishina Center, 2-1 Hirosawa, Wako, Saitama 351-0198, Japan*
[3]*Center for Nuclear Study, University of Tokyo, 7-3-1 Hongo, Bunkyo, Tokyo 113-0033, Japan*
[4]*School of Physics, Sichuan University, Chengdu 610065, China*
[5]*Department of Physics and Joint Institute for Nuclear Astrophysics, University of Notre Dame,
Nieuwland Science Hall, Notre Dame, Indiana 46556-5670, USA*
[6]*Department of Physics, Kyoto University, Kitashirakawa, Oiwakecho, Sakyo, Kyoto 606-8502, Japan*
[7]*Center for Mathematics and Physics, University of Aizu, Aizu-Wakamatsu, Fukushima 965-8560, Japan*
[8]*National Superconducting Cyclotron Laboratory, Michigan State University, East Lansing, Michigan 48824, USA*
(Received 23 March 2012; published 29 June 2012)

The double-differential cross sections for the ^{208}Pb and ^{90}Zr($t, ^3$He) reactions at 300 MeV/u have been measured at the RI Beam Factory at RIKEN. This was the first physics experiment with the SHARAQ magnetic spectrometer. The combined analysis of the present ($t, ^3$He) data and previous (n, p) data provides the clearest identification for the β^+ isovector spin monopole resonance both in the ^{208}Tl and ^{90}Y nuclei, and puts the observations of this giant resonance on a firm foundation. The measured distributions of the ($t, ^3$He) monopole cross sections were well reproduced by the distorted-wave Born approximation calculation, where the target transition density was calculated with the self-consistent Hartree-Fock plus random-phase approximation using the T43 Skyrme interaction. A major part of the expected β^+ isovector spin monopole strength was found in the measured cross section spectra.

Giant resonances (GRs) [1] in atomic nuclei are interesting examples of collective excitations in finite quantum many-body systems. In a macroscopic picture, GRs are regarded as collective excitations in coordinate, spin, and isospin space, whose signatures can be related to bulk properties of nuclei. Microscopically, GRs are described as coherent superpositions of $1p$ (particle)-$1h$ (hole) excitations. With the advent of modern rare isotope beam facilities, the study of GRs in unstable nuclei has been initiated (see, e.g., Refs. [2–4]). However, such facilities also provide new probes to study GRs in stable nuclei, the understanding of which is still poor. Here we report the identification of the β^+ isovector spin monopole resonance (IVSMR) via the ^{208}Pb and ^{90}Zr($t, ^3$He) reactions, utilizing a secondary triton beam at 300 MeV/u.

The IVSMR is an important topic in the study of charge-exchange spin-flip excitations in nuclei [5–7]. The isovector spin monopole (IVSM) operator is given by $O_{\mathrm{SM}}^{\pm} = \sum_i r_i^2 \boldsymbol{\sigma}_i t_i^{\pm}$, which induces the quantum-number changes of $\Delta L = 0$, $\Delta S = 1$, and $\Delta T = 1$. The Gamow-Teller (GT) operator has almost the same selection rule, but the GT operator induces $\Delta n = 0$ ($0\hbar\omega$) excitations while the IVSM transition is associated with $\Delta n = 1$ ($2\hbar\omega$) excitations. Here, n is the number of radial nodes of the single-particle wave function. Accurate data on the IVSMR would

provide crucial tests of microscopic calculations with effective nucleon-nucleon (N-N) interactions [5]. In addition, the development of tools to study the IVSMR provides a new method to determine the neutron-skin thickness in nuclei through the IVSM sum rule $S_- - S_+ = 3[N\langle r_n^4 \rangle - Z\langle r_p^4 \rangle]$ [5], where $S_-(S_+)$ refers to the total transition strength associated with the IVSMR in the β^- (β^+) direction. Its fourth-power dependence on the neutron (proton) radii r_n (r_p) makes it sensitive to the properties of the nuclear surface.

It has been established that spin-isospin modes can be selectively excited by charge-exchange reactions at intermediate energies [8,9]. Although nucleonic probes [(n, p) and (p, n)] have been used on a wide variety of isovector excitations, they are not suited to studying the IVSMR. The transition density associated with the IVSMR has a node near the nuclear surface. Since nucleonic probes penetrate deeply into the nuclear interior, transition amplitudes between the inner and outer parts of the transition density cancel, strongly reducing the cross section [10]. It was pointed out [11] that in order to strongly excite the IVSMR one needs absorptive projectiles like ^{3}He or tritons, which do not penetrate deeply into the nucleus and are sensitive only to the surface region. Therefore, it is advantageous to use the ($t, ^3$He) and (^{3}He, t) probes instead of the (n, p) and (p, n) probes.

Since the GT and IVSM excitations are both associated with $\Delta L = 0$, their differential cross sections are expected to have similar angular distributions. However, the difference in sensitivity for the excitation of the IVSMR between nucleon and nuclear probes can be used to distinguish the IVSMR from the GT "background." For example, in comparison to the excitation energy spectrum obtained in an (n, p) experiment, an enhancement is expected in the same spectrum obtained in a $(t, {}^3\text{He})$ experiment due to the stronger excitation of the IVSMR.

The first experimental signature of the IVSMR(β^-) was found in $({}^3\text{He}, t)$ data at 300 MeV/u [12]. Brockstedt *et al.* compared the $({}^3\text{He}, t)$ cross section at 300 MeV/u with the (p, n) cross section at 200 MeV and found significant enhancements of the former spectra at an excitation energy of about 30 MeV for the target nuclei ${}^{54}\text{Fe}$, ${}^{90}\text{Zr}$, and ${}^{208}\text{Pb}$. They could be partially attributed to the IVSMR(β^-), although this was not explicitly mentioned in Ref. [12]. In comparison with (p, n) data at 200 MeV, a possible enhancement due to the excitation of the IVSMR was also observed in a (p, n) experiment at 795 MeV [6], reflecting the fact that nucleonic probes also become absorptive at such high energies. Further evidence for the existence of the IVSMR in the β^- direction was found in a study of the ${}^{208}\text{Pb}({}^3\text{He}, tp)$ reaction at 140 MeV/u [7].

These experiments populated β^--type excitations. At TRIUMF [13,14], β^+-type excitations were investigated by comparing measured cross sections of ${}^{208}\text{Pb}(n, p)$ reactions at 458 and 198 MeV. Although a bump was found around $E_x = 13.6$ MeV, its multipolarity was not clearly determined. More recently, indications for the excitation of the IVSMR were found in the ${}^{48}\text{Ca}$ and ${}^{58}\text{Ni}(t, {}^3\text{He})$ reactions at 43 MeV/u [15] and the ${}^{150}\text{Sm}(t, {}^3\text{He})$ reaction at 115 MeV/u [16]. In this work, in order to identify the IVSMR(β^+) clearly, we measured double-differential cross sections of the $(t, {}^3\text{He})$ reaction at 300 MeV/u on the target nuclei ${}^{208}\text{Pb}$ and ${}^{90}\text{Zr}$, and distinguished the GT and IVSM components by comparing the obtained $(t, {}^3\text{He})$ spectra with previous (n, p) spectra [17,18].

The experiment was performed at the RI Beam Factory (RIBF) [19] at RIKEN, a unique facility capable of providing an intense triton beam at 300 MeV/u. The primary ${}^4\text{He}$ beam was accelerated to 320 MeV/u and bombarded onto a ${}^9\text{Be}$ production target with a thickness of 4 cm. From a variety of resulting fragments, tritons at 300 MeV/u were selected in the fragment separator BigRIPS [20]. The secondary triton beam was then achromatically transported to the secondary target. The beam spot at this target was 3 mm in diameter. It had an energy (angular) spread of 1.8 MeV (0.4°) at FWHM. The secondary targets included the isotopically enriched ${}^{208}\text{Pb}$ (98.4%) and ${}^{90}\text{Zr}$ (99.36%) targets with thicknesses of 400 and 308 mg/cm^2, respectively. An empty target frame and CH_2 targets were also installed for background and calibration measurements, respectively. The reaction products from the secondary

target were momentum analyzed by the SHARAQ magnetic spectrometer [21], and detected by two cathode-readout drift chambers and plastic scintillation counters installed at the final focal plane of the spectrometer. This was the first physics experiment with the SHARAQ spectrometer. The intensity of the secondary beam was indirectly monitored by a plastic counter installed 50 cm downstream of the secondary target. The primary beam intensity was approximately 300 pnA at the production target. The intensity of the secondary triton beam was 10^7 pps and its purity was in excess of 99%.

Scattering angles and momenta of the ${}^3\text{He}$ particles at the target were reconstructed from positions and angles measured in the focal plane of the SHARAQ spectrometer using a ray-trace procedure. The parameters for the ray-trace matrix were determined in a calibration measurement using the $CH_2(t, {}^3\text{He})$ reaction. The excitation energy, measured from the ground state of the daughter nuclei, was determined by means of the missing-mass method. The double-differential cross sections were determined for excitation energies of $0 \leq E_x \leq 40$ MeV and for scattering angles of $0° \leq \theta \leq 4°$. The background measured with an empty target frame was negligibly small ($\ll 1\%$) compared to the spectra with a target. The background due to hydrogen contamination of the ${}^{90}\text{Zr}$ target was evaluated and subtracted by using the corresponding peak in the $CH_2(t, {}^3\text{He})$ spectra.

Figure 1 presents the double-differential cross sections as a function of excitation energy at typical scattering angles for the ${}^{208}\text{Pb}(t, {}^3\text{He})$ (left) and ${}^{90}\text{Zr}(t, {}^3\text{He})$ (right) reactions, respectively. The spectra are shown with 1-MeV wide excitation energy bins in the top panels and 2-MeV bins in the others. The excitation-energy and scattering-angle resolutions were 2.5 MeV and 0.5° at FWHM, respectively. The statistical error was typically 3% per 1-MeV wide excitation energy bin and 0.4° wide scattering angle bin. The systematic error was estimated to be 7%, mainly originating from the uncertainties in the target thickness (5%) and the ray-trace matrix of the spectrometer (4%).

In order to extract the monopole component, we performed a multipole-decomposition (MD) analysis [8,18,22,23]. The method used in this analysis was similar to the one used in Ref. [8]. First, the angular distributions of the cross section were calculated for 1p-1h configurations with various multipoles using the distorted-wave Born approximation (DWBA) code FOLD [24]. The experimental angular distributions (0.4° bins, 9 angular points) in each 2-MeV wide energy bin were then fitted by a linear combination of theoretical angular distributions belonging to these multipoles. The following parameters were used in the FOLD calculations. The transition densities for the target and projectile systems were double folded over the effective N-N interaction at 325 MeV of Ref. [25]. The wave functions for the triton and ${}^3\text{He}$ particles were taken from variational Monte Carlo calculations [26]. For
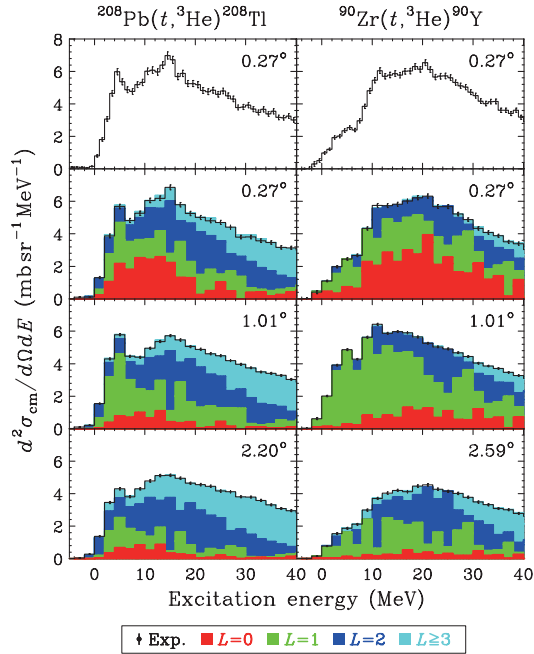
FIG. 1 (color). [Top] The cross section spectra at 0.27° in 1-MeV bins. The error bars include statistical errors only. The excitation energy is measured from the ground state of the daughter nuclei. [Others] The cross section spectra and the results of the MD analysis in 2-MeV bins. The monopole cross section spreads over a wide excitation energy region.

the target transition densities, single-particle wave functions were generated from the Woods-Saxon potential. The configurations taken into account were pure $1p$-$1h$ transitions with $\Delta J^\pi = 1^+ (\Delta L = 0)$, 0^-, 1^-, 2^- ($\Delta L = 1$), 3^+ ($\Delta L = 2$), 4^- ($\Delta L = 3$), and 5^+ ($\Delta L = 4$), which are within $2\hbar\omega$ excitations and not Pauli-blocked in the independent-particle model. GT transitions due to ground-state correlations were also taken into account. Optical potential (OP) parameters were generated by doubly folding the CEG07b G-matrix interaction [27].

The results of the MD analysis are also shown in Fig. 1. The red histograms represent the monopole ($\Delta L = 0$) components, which are populated over a wide excitation-energy region both in ^{208}Pb and ^{90}Zr. It can be seen that the monopole cross section in ^{208}Pb appears at a lower excitation energy compared to ^{90}Zr. The mass-number dependence of the excitation energy will be discussed below. The integrated monopole cross sections are 48 ± 3(syst) $\pm$ 3(stat) ± 3(MD) mb/sr for ^{208}Pb and 77 ± 5(syst) $\pm$ 4(stat) ± 4(MD) mb/sr for ^{90}Zr up to $E_x = 40$ MeV at $0°$. The statistical error of the MD analysis was determined by a Monte Carlo calculation, where the experimental data were randomly varied according to their statistical error, and the deviation of the resulting monopole cross section was determined. The error labeled "MD" includes the uncertainty in the OP and the N-N effective interaction.

The obtained monopole cross section contains both the GT and the IVSM components. In order to distinguish the

IVSM transitions from the GT transitions, we compared the monopole cross sections of our $(t, {}^3\text{He})$ and previous (n, p) spectra. If the (n, p) cross section is normalized so that it contains the same amount of the GT cross section as the $(t, {}^3\text{He})$ spectra, the IVSMR should appear as an enhancement for the $(t, {}^3\text{He})$ spectra compared with the normalized (n, p) spectra.

We used the ^{208}Pb(n, p) spectra at 200 MeV measured at TRIUMF [17] and the ^{90}Zr(n, p) spectra at 300 MeV measured at RCNP [18]. First these spectra were smeared, so that the difference of the energy resolutions between the $(t, {}^3\text{He})$ and (n, p) spectra was taken into account. The smeared spectra were then analyzed in the same way as the present MD analysis. The OP parameters for neutrons and protons were taken from Refs. [28,29], respectively. Because the number of data points is limited in the TRIUMF ^{208}Pb(n, p) spectra, transitions with $J^\pi = 2^-$ were excluded in the MD analysis. This can be justified because the strength of the 2^- transition is expected to be smaller than that of the 0^- and 1^- transitions, according to theoretical calculations [30]. Finally, the obtained monopole cross section was normalized by the GT cross section ratio (R_{GT}) of the $({}^3\text{He}, t)$ and (p, n) reactions taken from Ref. [12], assuming similarity of the β^- and β^+ reactions. In Ref. [12], the R_{GT} values between the $({}^3\text{He}, t)$ reaction at 300 MeV$/u$ and the (p, n) reaction at 200 MeV were determined as 1.57 for ^{208}Pb and 1.83 for ^{90}Zr. The incident-energy dependence of the (n, p) cross sections was also corrected by using the systematic studies of the GT unit cross section presented in Ref. [31].

The results are shown in the top panels of Fig. 2. At low excitation energies up to 5 MeV, the $(t, {}^3\text{He})$ cross sections were similar to the normalized (n, p) cross sections.
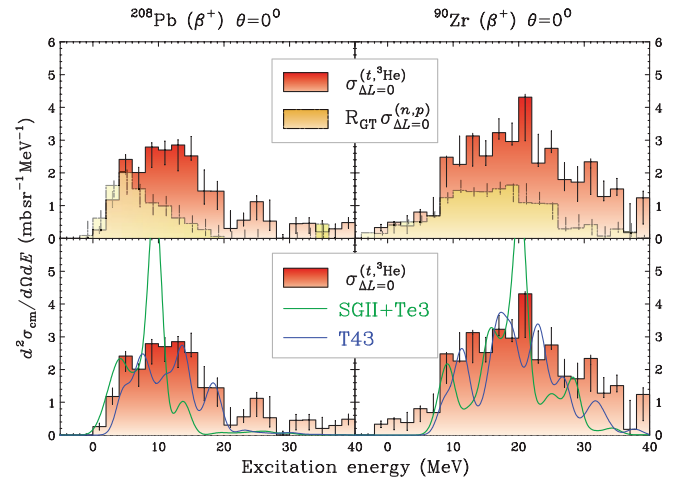

FIG. 2 (color). [Top] Comparison of the monopole cross section of the $(t, {}^3\text{He})$ and (n, p) spectra at $0°$. The (n, p) spectra were taken from Refs. [17,18]. [Bottom] Comparison of the $(t, {}^3\text{He})$ monopole cross sections of the experimental data and the DWBA + HF-RPA calculations. Only statistical errors are shown.

This implies that the monopole cross section in this region is dominated by GT transitions. On the other hand, at higher excitation energies, significant enhancements can be seen in the $(t, {}^3\text{He})$ spectra both for ${}^{208}\text{Pb}$ and ${}^{90}\text{Zr}$ targets. These enhancements can be attributed to the stronger excitations of the IVSMR in the $(t, {}^3\text{He})$ reaction.

We note that the comparison between the $(t, {}^3\text{He})$ and (n, p) spectra for the ${}^{208}\text{Pb}$ target is complicated by the fact that the velocities of the tritons and neutrons in the two experiments are not equal. Therefore, the momentum transfer q, for given excitation energy in ${}^{208}\text{Tl}$, is slightly different in the two experiments. Based on the DWBA calculations, we estimate that this could affect the comparison between the cross sections by a factor of 1.2 at $E_x = 5$ MeV and 1.7 at 15 MeV. The correction factor is a monotonic function of the excitation energy. Although this correction reduces the enhancement, a significant amount of enhancement still can be identified.

Our experimental data can also provide a test of theoretical calculations. The bottom panels in Fig. 2 represent comparisons between the experimental data and theoretical calculations on the $(t, {}^3\text{He})$ monopole cross section. The calculations were performed by using FOLD with almost the same parameters as those used in the MD analysis, except for the target transition densities. They were obtained by the fully self-consistent Hartree-Fock plus random-phase approximation (HF-RPA) calculation using the Skyrme effective interaction SGII + Te3 [32] and T43 [33]. Note that, in a previous work [32], the calculations with these interactions successfully reproduced the experimental centroid energies of the GT$^-$ and SD$^-$ (spin-dipole) strength distributions in ${}^{208}\text{Pb}$ and ${}^{90}\text{Zr}$. In this work, the DWBA calculation was performed for each transition density of $J^\pi = 1^+(\Delta L = 0)$ excitation, and the cross section at 0° was determined. The transition density included both GT and IVSM responses, and the interference effect between them was taken into account in this calculation. The excitation-energy spectra were then smeared with the experimental resolution. The green and blue lines in Fig. 2 represent the results using SGII + Te3 and T43, respectively. The calculation using SGII + Te3 shows a concentration of the cross section in a narrow region and does not reproduce the experimental data. However, the T43 calculation reproduces the cross section distribution well.

The integrated cross sections of the T43 calculation are 30 mb/sr for ${}^{208}\text{Pb}$ and 51 mb/sr for ${}^{90}\text{Zr}$ up to 40 MeV. The experimental cross sections amount to 160% and 151% of the calculated values, respectively. Those exceeding values can be attributed to uncertainties in the calculation. Because of the absorption effect, the cross section strongly depends on the overlap between the target transition density (ρ_{tr}^T) and the imaginary part (V_i) of the OP. For example, if the radial distribution of V_i is scaled by $+10\%$ with ρ_{tr}^T kept constant, the calculated cross section is decreased by -50% for ${}^{208}\text{Pb}$ and -40% for ${}^{90}\text{Zr}$. Even
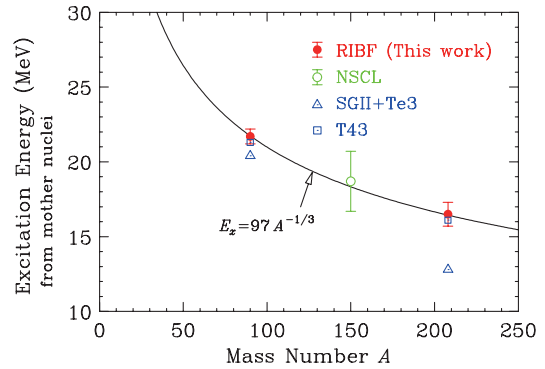

FIG. 3 (color). Systematics of the average energy of the monopole cross section distributions (see text). The excitation energy is measured from the ground state of the mother nuclei. The NSCL result [16] was obtained with an extrapolation to $q = 0$.

though there are uncertainties in the calculations, it is still possible to conclude that a major part of the expected IVSM strength was discovered in our $(t, {}^3\text{He})$ spectra.

Lastly, the excitation energy of the monopole cross section as a function of the mass number A is plotted in Fig. 3. The excitation energy is measured from the ground state of the mother nuclei in this discussion. The filled circles represent the average energies of the $\Delta L = 0$ cross sections in our $(t, {}^3\text{He})$ spectra. They are 16.5 ± 0.8 MeV (stat) for ${}^{208}\text{Pb}$ and 21.7 ± 0.5 MeV (stat) for ${}^{90}\text{Zr}$. For ${}^{208}\text{Pb}$ the average energy was calculated below 30 MeV and the high-energy tail was excluded. The data are fitted with a simple $A^{-1/3}$ dependence. The obtained function is $E_x = 97A^{-1/3}$, which is shown as a solid curve in Fig. 3. This is larger than the typical $2\hbar\omega$ value of $80A^{-1/3}$ [34], which is consistent with the repulsive nature of the spin-isospin part of the residual interaction. The result of the previous ${}^{150}\text{Sm}(t, {}^3\text{He})$ experiment [16] at NSCL is also shown as an open circle, which is in agreement with the fitted $A^{-1/3}$ dependence. The open triangle and square represent the theoretical results with the SGII + Te3 and T43 interactions, respectively. This shows again that the T43 calculation agrees better with the experimental data.

In summary, we have measured the double-differential cross sections of the ${}^{208}\text{Pb}$ and ${}^{90}\text{Zr}(t, {}^3\text{He})$ reactions at 300 MeV/u using the SHARAQ spectrometer. The monopole cross sections extracted from our $(t, {}^3\text{He})$ spectra were found to significantly exceed those of the previous (n, p) spectra. The absorptive nature of the $(t, {}^3\text{He})$ reaction allowed us to identify these enhancements as the IVSMRs (β^+). The $(t, {}^3\text{He})$ monopole cross sections were well reproduced by the DWBA + HF-RPA calculation with the effective interaction T43.

This experiment was performed at RIBF operated by RIKEN Nishina Center and CNS, University of Tokyo. The authors are grateful to I. Hamamoto and A. Tamii for valuable discussions. They also appreciate the efforts of T. Furumoto for providing the OP parameters. This work is

*miki@rcnp.osaka-u.ac.jp

†Present address: Research Center for Nuclear Physics, Osaka University, Mihogaoka, Ibaraki 567-0047, Japan.

[1] M. N. Harakeh and A. van der Woude, *Giant Resonances* (Oxford University, New York, 2001).

[2] M. N. Harakeh, Eur. Phys. J. A **13,** 169 (2002).

[3] P. Adrich *et al.*, Phys. Rev. Lett. **95,** 132501 (2005).

[4] C. Monrozeau *et al.*, Phys. Rev. Lett. **100,** 042501 (2008).

[5] I. Hamamoto and H. Sagawa, Phys. Rev. C **62,** 024319 (2000).

[6] D. Prout *et al.*, Phys. Rev. C **63,** 014603 (2000).

[7] R. G. T. Zegers *et al.*, Phys. Rev. Lett. **90,** 202501 (2003).

[8] M. Ichimura, H. Sakai, and T. Wakasa, Prog. Part. Nucl. Phys. **56,** 446 (2006).

[9] T. N. Taddeucci, C. A. Goulding, T. A. Carey, R. C. Byrd, C. D. Goodman, C. Gaarde, J. Larsen, D. Horen, J. Rapaport, and E. Sugarbaker, Nucl. Phys. **A469,** 125 (1987).

[10] N. Auerbach, Comments Nucl. Part. Phys. **22,** 223 (1998).

[11] N. Auerbach, F. Osterfeld, and T. Udagawa, Phys. Lett. B **219,** 184 (1989).

[12] A. Brockstedt *et al.*, Nucl. Phys. **A530,** 571 (1991).

[13] M. A. Moinester *et al.*, Phys. Lett. B **230,** 41 (1989).

[14] S. A. Long *et al.*, Phys. Rev. C **57,** 3191 (1998).

[15] J. Guillot *et al.*, Phys. Rev. C **73,** 014616 (2006).

[16] C. J. Guess *et al.*, Phys. Rev. C **83,** 064318 (2011).

[17] K. J. Raywood, S. A. Long, and B. M. Spicer, Nucl. Phys. **A625,** 675 (1997).

[18] K. Yako *et al.*, Phys. Lett. B **615,** 193 (2005).

[19] Y. Yano, Nucl. Instrum. Methods Phys. Res., Sect. B **261,** 1009 (2007).

[20] T. Kubo, Nucl. Instrum. Methods Phys. Res., Sect. B **204,** 97 (2003).

[21] T. Uesaka, S. Shimoura, H. Sakai, G. P. A. Berg, K. Nakanishi, Y. Sasamoto, A. Saito, S. Michimasa, T. Kawabata, and T. Kubo, Nucl. Instrum. Methods Phys. Res., Sect. B **266,** 4218 (2008).

[22] T. Wakasa *et al.*, Phys. Rev. C **55,** 2909 (1997).

[23] K. Yako *et al.*, Phys. Rev. Lett. **103,** 012503 (2009).

[24] J. Cook and J. A. Carr, computer program FOLD, Florida State University (unpublished); based on F. Petrovich and D. Stanley, Nucl. Phys. **A275,** 487 (1977); modified as described in J. Cook, K. W. Kemper , P. V. Drumm, L. K. Fifield, M. A. C. Hotchkis, T. R. Ophel, and C. L. Woods , Phys. Rev. C **30,** 1538 (1984); R. G. T. Zegers, S. Fracasso, and G. Colò, (unpublished).

[25] M. A. Franey and W. G. Love, Phys. Rev. C **31,** 488 (1985).

[26] S. C. Pieper and R. B. Wiringa, Annu. Rev. Nucl. Part. Sci. **51,** 53 (2001).

[27] T. Furumoto, Y. Sakuragi, and Y. Yamamoto, Phys. Rev. C **82,** 044612 (2010).

[28] Q.-b. Shen, D.-c. Feng, and Y.-z. Zhuo, Phys. Rev. C **43,** 2773 (1991).

[29] E. D. Cooper, S. Hama, B. C. Clark, and R. L. Mercer, Phys. Rev. C **47,** 297 (1993).

[30] N. Auerbach and A. Klein, Phys. Rev. C **30,** 1032 (1984).

[31] M. Sasano *et al.*, Phys. Rev. C **79,** 024602 (2009).

[32] C. L. Bai, H. Q. Zhang, H. Sagawa, X. Z. Zhang, G. Colò, and F. R. Xu, Phys. Rev. C **83,** 054316 (2011).

[33] T. Lesinski, M. Bender, K. Bennaceur, T. Duguet, and J. Meyer, Phys. Rev. C **76,** 014312 (2007).

[34] A. Bohr and B. R. Mottelson, *Nuclear Structure* (Benjamin, New York, 1969), Volume I–II.